JOURNAL OF MOLECULAR SPECTROSCOPY **169**, 410–420 (1995)

# Infrared Emission Spectra of InH and InD

J. B. WHITE, M. DULICK, AND P. F. BERNATH

*Centre for Molecular Beams and Laser Chemistry, Department of Chemistry, University of Waterloo, Waterloo, Ontario N2L 3G1, Canada*

High-resolution infrared emission spectra of diatomic indium hydride and deuteride were recorded with a Fourier transform spectrometer. A total of 377 InH lines from the (1, 0) to (5, 4) bands and 257 InD lines from the (1, 0) to (4, 3) bands were measured. Revised sets of isotopically dependent Dunham $Y$ constants and isotopically invariant Dunham $U$ constants for the $X\,^1\Sigma^+$ ground state were determined. In addition, a parametrized internuclear potential for the $X\,^1\Sigma^+$ state was also obtained from a direct fit of the data to the eigenvalues of the radial Schrödinger equation. 

## 1. INTRODUCTION

The first electronic spectrum of InH was recorded in emission by Grundström in 1938 (*1, 2*); he identified two electronic transitions and assigned them as $\Sigma-\Sigma$ and $\Pi-\Sigma$ from a rotational analysis of bands in the 5650–7250 Å region. Subsequent investigations by Kleman (*3*), Neuhaus (*4, 5*), and Ginter (*6, 7*) have since proven that the visible bands observed by Grundström are actually from the intercombination transition, $a\,^3\Pi-X\,^1\Sigma^+$. Neuhaus (*4, 5*) also discovered a second electronic transition, $A\,^1\Pi-X\,^1\Sigma^+$, in the 4400–4900 Å region of the absorption spectrum, thereby accounting for three of the four possible low-lying electronic states, $^1\Sigma^+$, $^3\Pi$, $^1\Pi$, and $^3\Sigma^+$, formed from the atomic states $\mathrm{In}(^2P) + \mathrm{H}(^2S)$.

Most of the early interest in InH(InD) was focused on the first excited state, $a\,^3\Pi$. Predissociation has been observed in the rotational levels of all the $a\,^3\Pi$ substates (*1–7*). An RKR analysis by Ginter and Battino (*8*) indicated that the potential curves for the $a\,^3\Pi_{0,1,2}$ substates are anomalous and even suggested the possibility of the existence of a local maximum in the $a\,^3\Pi_1$ potential curve at $R \sim 3.3$ Å. The large and asymmetric spin–orbit splittings of the $a\,^3\Pi$ substates and the 50-$\mathrm{cm}^{-1}$ splitting between $a\,^3\Pi_{0^+}$ and $a\,^3\Pi_{0^-}$ prompted Veseth and Lofthus (*9*) to fit the rotational structure of these substates to the levels of a Hund's case $c$ Hamiltonian. Neuhaus and co-workers (*10, 11*) also observed under Doppler-limited conditions resolved hyperfine splittings in lowest-$J$ $P$, $Q$, and $R$ lines from the InH (0, 0) and (1, 1) bands as well as the InD (0, 0) band of $^3\Pi_1-{}^1\Sigma^+$. Analysis of the $a\,^3\Pi$ hyperfine structure was first attempted by Mustelin (*12*) and later reanalyzed by Freed (*13*) with a $c_\beta$ Hamiltonian model and finally by Veseth (*14*) with a $c_\alpha$ Hamiltonian model.

To date only two ab initio calculations have been reported so far on InH, the CI relativistic pseudopotential calculation by Teichteil and Spiegelmann (*15*) and the MCSCF(CASSCF) calculation by Balasubramanian (*16*).

The only published rotation-vibration spectra for the $X\,^1\Sigma^+$ ground state are the diode laser measurements on InH by Bahnmaier *et al.* (*17*) and on InD by Urban *et al.* (*18*). Because of the limited wavelength coverage of a diode laser, a relatively small number of rotational lines (<100) were measured in the fundamental and hot bands of either InH or InD.

0022-2852/95 $6.00

As part of our continuing investigation on the infrared spectroscopy of the diatomic Group III hydrides and deuterides, we report here on the high-resolution infrared emission spectra of InH and InD recorded with a Fourier transform spectrometer. The wide and continuous spectral coverage afforded by this technique allowed us to measure almost 300 lines in both the hydride and deteuride spectra which span the region 800–1600 $cm^{-1}$.

## 2. EXPERIMENTAL DETAILS

The InH and InD high-resolution spectra were recorded with a Bruker IFS 120 Fourier transform spectrometer. Except for some minor changes, essentially the same operating conditions and procedures were followed in recording these spectra as described in the earlier papers on AlH–AlD (*19*) and GaH–GaD (*20*). Because indium attains a higher vapor pressure at a much lower temperature as compared to aluminum and gallium, all the scans were recorded at a temperature of 1200°C. The final InH(InD) spectrum was obtained by transforming an interferogram assembled from 50 individual scans where each scan was recorded at a resolution of 0.006 $cm^{-1}$.

Rotational line centers were determined using Brault's computer program PC-DECOMP which fits measured spectral line profiles to Voigt lineshape functions. The presence of impurity $CD_4$ (deteurated methane) lines in the InD spectrum was used in the absolute frequency calibration of the deuteride lines (*21*). The InH spectrum contained both weak InD emission lines and $H_2O$ absorption lines. However, the $H_2O$ lines were much too broad to be useful in calibrating the spectrum. The weaker but narrower InD lines were chosen instead to calibrate the frequency scale of the InH spectrum.

A total of 377 InH lines from the (1, 0) to (5, 4) bands and 257 InD lines from the (1, 0) to (4, 3) bands were measured from their respective spectra. Naturally occurring indium consists of two isotopes, $^{113}In$ and $^{115}In$, with abundances of 4.3 and 95.7%, respectively (*22*). Consequently, 75% of the hydride lines and 95% of the deuteride lines measured involved the $^{115}In$ isotope. The complete list of measured hydride and deuteride lines is given in Tables I–IV.

The line positions for the strong and sharp hydride lines in the InH spectrum with a signal-to-noise ratio $\geqslant 100$ were measured to a precision of $\pm 0.0002$ $cm^{-1}$, while the precision for the remainder of weak lines were more typically on the order of $\pm 0.0005$ $cm^{-1}$. In contrast, the overall quality of the InD spectrum was generally much poorer due to a higher and noisier background where the signal-to-noise ratio for even the best deuteride lines was <50. Our assessment is that the InD line positions are measured to no better than $\pm 0.0005$ $cm^{-1}$ for the sharpest and most intense lines and $\pm 0.005$ $cm^{-1}$ for the weaker lines. It is also important to note that because the InH lines were calibrated relative to the best InD lines, the absolute precision of the hydride line positions can be no better than $\pm 0.0005$ $cm^{-1}$.

## 3. RESULTS AND DISCUSSION

### *3.1. Dunham Fits*

Three sets of Dunham molecular constants for the $X^1\Sigma^+$ state were determined from the data analysis. The conventional isotopically dependent Dunham $Y$ constants, listed in Table V for $^{115}InH$ and $^{115}InD$, were obtained by fitting the data of each isotopomer separately to the energy level expression (*23*)

TABLE I

Observed Lines of $^{115}$InH

| Line | Observed | Δ | Line | Observed | Δ | Line | Observed | Δ | Line | Observed | Δ |
|---|---|---|---|---|---|---|---|---|---|---|---|
| | | | | | (1, 0) Band | | | | | | |
| P(36) | 939.3697 | -103 | P(35) | 955.2877 | -12 | P(34) | 971.1334 | -12 | P(33) | 986.9102 | -4 |
| P(32) | 1002.6107 | 1 | P(31) | 1018.2281 | -2 | P(30) | 1033.7571 | 1 | P(29) | 1049.1902 | -1 |
| P(28) | 1064.5224 | 6 | P(27) | 1079.7449 | 3 | P(26) | 1094.8527 | 3 | P(25) | 1109.8386 | -1 |
| P(24) | 1124.6964 | -1 | P(23) | 1139.4193 | -3 | P(22) | 1154.0012 | 1 | P(21) | 1168.4350 | 5 |
| P(20) | 1182.7127 | -4 | P(19) | 1196.8304 | 0 | P(18) | 1210.7799 | 1 | P(17) | 1224.5545 | -3 |
| P(16) | 1238.1486 | -2 | P(15) | 1251.5555 | 3 | P(14) | 1264.7675 | -3 | P(13) | 1277.7799 | 0 |
| P(12) | 1290.5853 | 1 | P(11) | 1303.1776 | 2 | P(10) | 1315.5504 | 3 | P(9) | 1327.6971 | -1 |
| P(8) | 1339.6126 | 2 | P(7) | 1351.2893 | -4 | P(6) | 1362.7232 | 2 | P(5) | 1373.9062 | 0 |
| P(4) | 1384.8338 | 1 | P(3) | 1395.4998 | 3 | P(2) | 1405.8982 | 2 | P(1) | 1416.0232 | -2 |
| R(0) | 1435.4333 | 2 | R(1) | 1444.7073 | 7 | R(2) | 1453.6853 | -3 | R(3) | 1462.3650 | 0 |
| R(4) | 1470.7397 | 0 | R(5) | 1478.8048 | -1 | R(6) | 1486.5559 | 1 | R(7) | 1493.9879 | 0 |
| R(9) | 1507.8774 | -1 | R(10) | 1514.3263 | -1 | R(11) | 1520.4392 | -1 | R(12) | 1526.2122 | -1 |
| R(13) | 1531.6420 | 4 | R(14) | 1536.7229 | -4 | R(15) | 1541.4541 | -2 | R(16) | 1545.8313 | 1 |
| R(17) | 1549.8507 | 1 | R(18) | 1553.5098 | 1 | R(36) | 1555.3080 | 7 | R(19) | 1556.8056 | -1 |
| R(20) | 1559.7360 | 3 | R(34) | 1561.2311 | 9 | R(21) | 1562.2972 | -2 | R(33) | 1563.6123 | 5 |
| R(22) | 1564.4882 | -1 | R(32) | 1565.6078 | 7 | R(23) | 1566.3063 | 1 | R(31) | 1567.2167 | 0 |
| R(24) | 1567.7493 | 0 | R(30) | 1568.4408 | -3 | R(25) | 1568.8157 | 3 | R(29) | 1569.2810 | 0 |
| R(26) | 1569.5032 | 0 | R(28) | 1569.7368 | -4 | R(27) | 1569.8110 | 1 | | | |
| | | | | | (2, 1) Band | | | | | | |
| P(35) | 919.6812 | 136 | P(34) | 935.1406 | 345 | P(33) | 950.4754 | 2 | P(32) | 965.7686 | 2 |
| P(31) | 980.9793 | -6 | P(30) | 996.1034 | 1 | P(29) | 1011.1326 | 1 | P(28) | 1026.0611 | -1 |
| P(27) | 1040.8834 | 2 | P(26) | 1055.5924 | 4 | P(25) | 1070.1816 | 2 | P(24) | 1084.6449 | 0 |
| P(23) | 1098.9758 | -3 | P(22) | 1113.1687 | -1 | P(21) | 1127.2161 | -1 | P(20) | 1141.1120 | -4 |
| P(19) | 1154.8504 | 0 | P(18) | 1168.4244 | 0 | P(17) | 1181.8276 | -1 | P(16) | 1195.0540 | 1 |
| P(15) | 1208.0971 | 2 | P(14) | 1220.9502 | 1 | P(13) | 1233.6075 | 0 | P(12) | 1246.0628 | 2 |
| P(11) | 1258.3098 | 3 | P(10) | 1270.3417 | 0 | P(9) | 1282.1537 | 2 | P(8) | 1293.7386 | 0 |
| P(7) | 1305.0912 | 1 | P(6) | 1316.2052 | 1 | P(5) | 1327.0739 | -8 | P(4) | 1337.6941 | -1 |
| P(3) | 1348.0581 | 4 | P(2) | 1358.1597 | -2 | P(1) | 1367.9943 | -9 | R(0) | 1386.8432 | -1 |
| R(1) | 1395.8457 | 3 | R(2) | 1404.5602 | 7 | R(3) | 1412.9808 | 2 | R(4) | 1421.1039 | 2 |
| R(5) | 1428.9241 | 2 | R(6) | 1436.4368 | 0 | R(7) | 1443.6378 | 1 | R(8) | 1450.5221 | 0 |
| R(9) | 1457.0860 | 3 | R(10) | 1463.3245 | -1 | R(11) | 1469.2345 | -1 | R(12) | 1474.8118 | 1 |
| R(13) | 1480.0524 | -1 | R(14) | 1484.9527 | -3 | R(15) | 1489.5104 | 4 | R(16) | 1493.7198 | -4 |
| R(17) | 1497.5805 | 1 | R(18) | 1501.0951 | 75 | R(19) | 1504.2386 | -3 | R(20) | 1507.0316 | -1 |
| R(21) | 1509.4632 | -2 | R(22) | 1511.5315 | -1 | R(32) | 1511.8070 | -3 | R(23) | 1513.2343 | 1 |
| R(31) | 1513.4711 | -5 | R(24) | 1514.5682 | -7 | R(30) | 1514.7576 | 7 | R(25) | 1515.5341 | 1 |
| R(29) | 1515.6642 | 3 | R(26) | 1516.1275 | -1 | R(28) | 1516.1940 | 1 | R(27) | 1516.3476 | -4 |

$$E(v, J) = \sum_{i,j} Y_{ij}\left(v + \frac{1}{2}\right)^i [J(J+1)]^j. \tag{1}$$

The standard deviations were 0.838 for the $^{115}$InH fit and 0.816 for the $^{115}$InD fit. Due to the lack of a sufficient number of lines, $Y$'s for minor isotopomers, $^{113}$InH and $^{113}$InD, were not determined by fitting the data to Eq. (1). Instead the $Y$'s listed in Table V for these minor isotopomers were calculated from the corresponding $Y$'s of the major isotopomers by using the relation

$$Y_{ij}(113) = \left(\frac{\mu(115)}{\mu(113)}\right)^{(i+2j)/2} Y_{ij}(115), \tag{2}$$

TABLE I—*Continued*

| Line | Observed | Δ | Line | Observed | Δ | Line | Observed | Δ | Line | Observed | Δ |
|---|---|---|---|---|---|---|---|---|---|---|---|
| | | | | | (3, 2) Band | | | | | | |
| P(29) | 973.8847 | -8 | P(28) | 988.4319 | 1 | P(27) | 1002.8623 | -101 | P(26) | 1017.2014 | 2 |
| P(25) | 1031.4125 | 5 | P(24) | 1045.4997 | 8 | P(23) | 1059.4563 | 7 | P(22) | 1073.2758 | -1 |
| P(21) | 1086.9535 | -2 | P(20) | 1100.4826 | 0 | P(19) | 1113.8566 | -1 | P(18) | 1127.0697 | 1 |
| P(17) | 1140.1154 | 2 | P(16) | 1152.9873 | 1 | P(15) | 1165.6795 | -1 | P(14) | 1178.1859 | -3 |
| P(13) | 1190.5007 | -1 | P(12) | 1202.6172 | -3 | P(11) | 1214.5305 | 3 | P(10) | 1226.2325 | -4 |
| P(9) | 1237.7193 | -3 | P(8) | 1248.9843 | -1 | P(7) | 1260.0216 | 3 | P(6) | 1270.8250 | 0 |
| P(5) | 1281.3893 | 0 | P(4) | 1291.7087 | -1 | P(3) | 1301.7779 | 0 | P(2) | 1311.5910 | -1 |
| P(1) | 1321.1405 | -24 | R(1) | 1348.1765 | -10 | R(2) | 1356.6317 | 0 | R(3) | 1364.7984 | -5 |
| R(4) | 1372.6741 | -2 | R(5) | 1380.2529 | -2 | R(6) | 1387.5314 | 5 | R(7) | 1394.5023 | -7 |
| R(8) | 1401.1654 | 3 | R(9) | 1407.5130 | -1 | R(10) | 1413.5427 | 1 | R(11) | 1419.2502 | 2 |
| R(12) | 1424.6307 | -5 | R(13) | 1429.6827 | 2 | R(14) | 1434.4004 | 0 | R(15) | 1438.7817 | 3 |
| R(16) | 1442.8227 | 4 | R(17) | 1446.5196 | -2 | R(18) | 1449.8709 | -1 | R(19) | 1452.8729 | 0 |
| R(20) | 1455.5232 | 3 | R(21) | 1457.8192 | 8 | R(32) | 1459.0651 | -3 | R(22) | 1459.7573 | 4 |
| R(31) | 1460.8015 | -3 | R(23) | 1461.3370 | 10 | R(30) | 1462.1657 | 16 | R(24) | 1462.5535 | -2 |
| R(29) | 1463.1553 | 19 | R(25) | 1463.4084 | 5 | R(28) | 1463.7711 | 2 | R(26) | 1463.8978 | 11 |
| R(27) | 1464.0192 | 10 | | | | | | | | | |
| | | | | | (4, 3) Band | | | | | | |
| P(26) | 979.5555 | -23 | P(24) | 1007.1371 | -4 | P(23) | 1020.7372 | -1 | P(22) | 1034.2044 | 21 |
| P(21) | 1047.5255 | -12 | P(20) | 1060.7045 | -1 | P(19) | 1073.7293 | -5 | P(18) | 1086.5966 | 1 |
| P(17) | 1099.2983 | -3 | P(16) | 1111.8299 | -2 | P(15) | 1124.1856 | 5 | P(14) | 1136.3579 | 2 |
| P(13) | 1148.3421 | 2 | P(12) | 1160.1316 | -2 | P(11) | 1171.7206 | -7 | P(10) | 1183.1060 | 11 |
| P(9) | 1194.2762 | -5 | P(8) | 1205.2299 | -10 | P(7) | 1215.9615 | -2 | P(6) | 1226.4632 | -5 |
| P(5) | 1236.7308 | -3 | P(4) | 1246.7578 | -6 | P(3) | 1256.5401 | -1 | P(2) | 1266.0700 | -11 |
| R(0) | 1293.1072 | 15 | R(1) | 1301.5830 | 21 | R(2) | 1309.7793 | -1 | R(3) | 1317.6978 | 13 |
| R(4) | 1325.3273 | -2 | R(5) | 1332.6673 | -4 | R(6) | 1339.7088 | -37 | R(7) | 1346.4572 | -3 |
| R(8) | 1352.8983 | -2 | R(9) | 1359.0319 | 7 | R(10) | 1364.8514 | -1 | R(11) | 1370.3558 | 3 |
| R(12) | 1375.5384 | -10 | R(13) | 1380.3992 | -1 | R(14) | 1384.9327 | 7 | R(15) | 1389.1334 | -2 |
| R(16) | 1393.0009 | -2 | R(17) | 1396.5315 | 3 | R(18) | 1399.7215 | 6 | R(19) | 1402.5675 | 4 |
| R(20) | 1405.0677 | 6 | R(21) | 1407.2188 | 5 | R(22) | 1409.0196 | 15 | R(23) | 1410.4633 | -6 |
| R(24) | 1411.5531 | -5 | R(25) | 1412.2856 | 5 | R(27) | 1412.6610 | -37 | | | |
| | | | | | (5, 4) Band | | | | | | |
| P(19) | 1034.3433 | -14 | P(18) | 1046.8862 | 62 | P(17) | 1059.2514 | -17 | P(16) | 1071.4588 | 10 |
| P(15) | 1083.4897 | 9 | P(14) | 1095.3408 | 7 | P(13) | 1107.0059 | 0 | P(12) | 1118.4817 | 12 |
| P(11) | 1129.7583 | 1 | P(10) | 1140.8348 | 14 | P(9) | 1151.6998 | -5 | P(8) | 1162.3523 | -10 |
| P(7) | 1172.7873 | 4 | P(6) | 1182.9960 | 3 | P(5) | 1192.9748 | 7 | P(4) | 1202.7190 | 24 |
| R(0) | 1247.7100 | 19 | R(2) | 1263.8878 | 149 | R(3) | 1271.5437 | 5 | R(4) | 1278.9333 | 10 |
| R(5) | 1286.0378 | 20 | R(6) | 1292.8492 | 1 | R(7) | 1299.3685 | 7 | R(8) | 1305.5870 | -8 |
| R(9) | 1311.5052 | 5 | R(10) | 1317.1146 | 0 | R(11) | 1322.4128 | -7 | R(12) | 1327.3955 | -21 |
| R(13) | 1332.0615 | -15 | R(14) | 1336.4041 | -22 | | | | | | |

which assumes negligible breakdown in the Born–Oppenheimer approximation on the indium center, as discussed below.

The isotopically invariant Dunham $U$ constants given in Table VI were determined by fitting the combined set of hydride and deuteride lines to

$$E(v, J) = \sum_{i,j} \mu^{-(i+2j)/2} U_{ij}[1 + (m_e/M_A)\Delta_{ij}^{A} + (m_e/M_B)\Delta_{ij}^{B}] \times \left(v + \frac{1}{2}\right)^{i} [J(J+1)]^{j}, \quad (3)$$

TABLE II

Observed Lines of $^{113}$InH

| Line | Observed | Δ | Line | Observed | Δ | Line | Observed | Δ | Line | Observed | Δ |
|---|---|---|---|---|---|---|---|---|---|---|---|
| | | | | | (1, 0) Band | | | | | | |
| P(36) | 939.3779 | -274 | P(30) | 1033.8332 | 353 | P(29) | 1049.2296 | -42 | P(28) | 1064.5651 | -26 |
| P(24) | 1124.7519 | -8 | P(23) | 1139.4782 | 0 | P(22) | 1154.0623 | 1 | P(21) | 1168.4959 | -21 |
| P(19) | 1196.8978 | -10 | P(18) | 1210.8500 | -6 | P(17) | 1224.6274 | -5 | P(16) | 1238.2242 | 1 |
| P(15) | 1251.6335 | 6 | P(14) | 1264.8473 | -3 | P(13) | 1277.8622 | 3 | P(12) | 1290.6683 | -11 |
| P(11) | 1303.2639 | 2 | P(10) | 1315.6381 | -3 | P(9) | 1327.7877 | 2 | P(8) | 1339.7088 | 41 |
| P(7) | 1351.3852 | 13 | P(6) | 1362.8183 | -8 | P(5) | 1374.0040 | -2 | P(4) | 1384.9327 | -7 |
| P(2) | 1406.0000 | -9 | P(1) | 1416.0924 | -355 | R(0) | 1435.5406 | 1 | R(1) | 1444.8196 | 42 |
| R(2) | 1453.7960 | 2 | R(3) | 1462.4761 | -3 | R(4) | 1470.8530 | 8 | R(5) | 1478.9172 | -13 |
| R(6) | 1486.6702 | -3 | R(7) | 1494.1035 | 0 | R(8) | 1501.2123 | -7 | R(9) | 1507.9954 | 7 |
| R(10) | 1514.4443 | 0 | R(11) | 1520.5581 | 1 | R(12) | 1526.3310 | -5 | R(13) | 1531.7606 | -6 |
| R(14) | 1536.8434 | 0 | R(15) | 1541.5738 | -9 | R(16) | 1545.9513 | -4 | R(17) | 1549.9710 | -2 |
| R(18) | 1553.6308 | 4 | R(19) | 1556.9271 | 8 | R(20) | 1559.8572 | 11 | R(21) | 1562.4160 | -16 |
| R(22) | 1564.6079 | -3 | R(23) | 1566.4264 | 7 | R(24) | 1567.8667 | -15 | | | |
| | | | | | (2, 1) Band | | | | | | |
| P(32) | 965.7789 | -207 | P(28) | 1026.0861 | -162 | P(27) | 1040.9254 | -14 | P(26) | 1055.6430 | 50 |
| P(25) | 1070.2282 | -16 | P(24) | 1084.6966 | 8 | P(21) | 1127.2701 | -41 | P(20) | 1141.1696 | -30 |
| P(19) | 1154.9116 | -14 | P(18) | 1168.4959 | 67 | P(17) | 1181.8959 | 12 | P(16) | 1195.1238 | 6 |
| P(15) | 1208.1682 | -1 | P(14) | 1221.0241 | 4 | P(13) | 1233.6839 | 7 | P(12) | 1246.1406 | 2 |
| P(11) | 1258.3890 | -2 | P(10) | 1270.4239 | 3 | P(9) | 1282.2375 | 3 | P(8) | 1293.8243 | 1 |
| P(7) | 1305.1792 | 7 | P(6) | 1316.2941 | -2 | P(5) | 1327.1650 | -6 | P(4) | 1337.7862 | -5 |
| P(3) | 1348.1765 | 245 | P(2) | 1358.2718 | 161 | R(2) | 1404.6635 | 13 | R(3) | 1413.0848 | 3 |
| R(4) | 1421.2102 | 15 | R(5) | 1429.0286 | -14 | R(6) | 1436.5440 | 2 | R(7) | 1443.7454 | -1 |
| R(8) | 1450.6309 | 2 | R(9) | 1457.1944 | -8 | R(10) | 1463.4343 | -4 | R(11) | 1469.3458 | 6 |
| R(12) | 1474.9225 | -4 | R(13) | 1480.1637 | -3 | R(14) | 1485.0638 | -12 | R(15) | 1489.6220 | -3 |
| R(16) | 1493.8318 | -7 | R(17) | 1497.6935 | 7 | R(18) | 1501.2123 | 122 | R(21) | 1509.5708 | -46 |
| R(22) | 1511.6415 | -18 | | | | | | | | | |

where the two atomic centers are labeled as A and B; $m_e$, $M$, and $\mu$ are the electron, atomic, and reduced masses; and $\Delta_{ij}^{A}$ and $\Delta_{ij}^{B}$ are Born–Oppenheimer breakdown constants (see Table VII) for atoms A and B (*24, 25*).

The set of Dunham $U$ values that appear in the column labeled "unconstrained" in Table VI were determined by treating all the $U$'s as adjustable parameters in the fit. The second set of $U$'s listed in the column labeled "constrained" were determined

TABLE III

Observed Lines of $^{113}$InD

| Line | Observed | Δ | Line | Observed | Δ | Line | Observed | Δ | Line | Observed | Δ |
|---|---|---|---|---|---|---|---|---|---|---|---|
| | | | | | (1, 0) Band | | | | | | |
| R(8) | 1063.8235 | -28 | R(9) | 1067.7387 | 5 | R(10) | 1071.5361 | 14 | R(11) | 1075.2129 | -16 |
| R(13) | 1082.2187 | -14 | R(15) | 1088.7737 | 278 | R(17) | 1094.7886 | 47 | R(18) | 1097.6157 | -18 |
| R(19) | 1100.3241 | -20 | R(20) | 1102.9030 | -59 | R(21) | 1105.3613 | -37 | R(22) | 1107.6970 | 34 |
| R(24) | 1111.9698 | 53 | | | | | | | | | |

by treating only the $U_{i0}$'s and $U_{i1}$'s as adjustable parameters and fixing all remaining $U_{ij}$'s for $j > 1$ to constraints which relate these $U$'s to the $U_{i0}$'s and $U_{i1}$'s (*26*). The standard deviation for the "unconstrained" and "constrained" fits were 0.972 and 1.124, respectively. The residuals obtained from the "constrained" fit are given in Tables I–IV.

In principle, the presence of $^{113}$InH(D) and $^{115}$InH(D) rotational lines in the spectrum provides a rare opportunity in determining $\Delta$'s for both atomic centers. However, our efforts to determine the effects of Born–Oppenheimer breakdown on the indium center were hampered by the limited number of recorded $^{113}$InH(D) lines, the absolute precision of the $^{113}$InD lines ($\pm 0.005$ cm$^{-1}$), and the insensitivity of Eq. (3) to the change in isotopic mass of the indium nucleus. Based partially on the analysis of the InF spectrum (*27*), we estimate that the upper bound on the relative shift between $^{113}$InH(D) and $^{115}$InH(D) $\Delta v = +1$ rotational lines due to Born–Oppenheimer breakdown on the indium center is probably less than 0.0005 cm$^{-1}$. As expected the only sizeable contribution of Born–Oppenheimer breakdown resides on the hydrogen center where, for example, seven $\Delta$'s were statistically well determined in the constrained fit.

### *3.2. Internuclear Potentials*

The final phase of the analysis involved determining an internuclear potential by fitting the data directly to the eigenvalues of the radial Schrödinger equation

$$\left\{\frac{\hbar^2}{2\mu}\nabla^2 - U^{\text{eff}}(R) + E(v, J) - \frac{\hbar^2}{2\mu}[1 + q(R)]J(J+1)/R^2\right\} \times \psi(r; v, J) = 0 \quad (4)$$

using an effective internuclear potential for vibrational motion of the form

$$U^{\text{eff}}(R) = U^{\text{BO}}(R) + U^{\text{C}}(R), \quad (5)$$

where

$$U^{\text{BO}} = D_e\{1 - \exp[-\beta(R)]\}^2/\{1 - \exp[\beta(\infty)]\}^2, \quad (6)$$

$$\beta(R) = z\sum_{i=0}\beta_i z^i, \quad (7)$$

and

$$z = (R - R_e)/(R + R_e). \quad (8)$$

Corrections for the breakdown in the Born–Oppenheimer approximation are represented by power series expansions. Specifically,

$$U^{\text{C}}(R) = M_{\text{A}}^{-1}\sum_{i=1} u_i^{\text{A}}(R - R_e)^i + M_{\text{B}}^{-1}\sum_{i=1} u_i^{\text{B}}(R - R_e)^i \quad (9)$$

approximates both the adiabatic correction and homogeneous nonadiabatic mixing terms in the nuclear part of the diatomic Hamiltonian, while

$$q(R) = M_{\text{A}}^{-1}\sum_{i=0} q_i^{\text{A}}(R - R_e)^i + M_{\text{B}}^{-1}\sum_{i=0} q_i^{\text{B}}(R - R_e)^i \quad (10)$$

takes into account heterogeneous nonadiabatic mixing.

Results from the parametrized potential fit are summarized in Table VIII which involved 19 adjustable parameters comprised of 9 $\beta$'s for the modified-Morse form of the Born–Oppenheimer potential and 5 $u$ and 4 $q$ power series expansion parameters

TABLE IV

Observed Lines of $^{115}$InD

| Line | Observed | Δ | Line | Observed | Δ | Line | Observed | Δ | Line | Observed | Δ |
|---|---|---|---|---|---|---|---|---|---|---|---|
| | | | | | (1, 0) Band | | | | | | |
| P(28) | 850.2695 | -1 | P(27) | 857.4598 | -1 | P(26) | 864.5889 | -13 | P(25) | 871.6577 | -8 |
| P(24) | 878.6637 | 3 | P(23) | 885.6030 | 0 | P(22) | 892.4755 | -3 | P(21) | 899.2797 | -3 |
| P(20) | 906.0147 | 6 | P(19) | 912.6764 | 1 | P(18) | 919.2649 | 0 | P(17) | 925.7788 | 4 |
| P(16) | 932.2154 | 3 | P(15) | 938.5735 | -1 | P(14) | 944.8524 | 6 | P(13) | 951.0488 | 2 |
| P(12) | 957.1621 | 0 | P(11) | 963.1910 | 1 | P(10) | 969.1342 | 9 | P(9) | 974.9879 | 0 |
| P(8) | 980.7532 | 3 | P(7) | 986.4277 | 6 | P(6) | 992.0085 | -4 | P(5) | 997.4967 | 1 |
| P(4) | 1002.8895 | 7 | P(3) | 1008.1842 | -1 | P(2) | 1013.3802 | -11 | P(1) | 1018.4792 | 6 |
| R(0) | 1028.3688 | 7 | R(1) | 1033.1614 | 37 | R(2) | 1037.8415 | -4 | R(3) | 1042.4201 | 6 |
| R(4) | 1046.8887 | -4 | R(5) | 1051.2495 | 0 | R(6) | 1055.4992 | -2 | R(7) | 1059.6372 | -2 |
| R(8) | 1063.6620 | -5 | R(9) | 1067.5733 | -1 | R(10) | 1071.3685 | -4 | R(11) | 1075.0481 | 2 |
| R(12) | 1078.6093 | 1 | R(13) | 1082.0514 | -3 | R(14) | 1085.3745 | 0 | R(15) | 1088.5763 | 1 |
| R(16) | 1091.6560 | -1 | R(17) | 1094.6129 | -1 | R(18) | 1097.4456 | -5 | R(19) | 1100.1544 | 2 |
| R(20) | 1102.7371 | 4 | R(21) | 1105.1926 | 2 | R(22) | 1107.5207 | 0 | R(23) | 1109.7209 | 3 |
| R(24) | 1111.7912 | -1 | R(25) | 1113.7326 | 4 | R(26) | 1115.5424 | 0 | R(27) | 1117.2220 | 9 |
| R(28) | 1118.7684 | 5 | R(29) | 1120.1821 | 2 | R(30) | 1121.4623 | -3 | R(31) | 1122.6094 | 0 |
| R(32) | 1123.6230 | 14 | R(33) | 1124.4998 | 9 | R(34) | 1125.2408 | 2 | R(35) | 1125.8472 | 8 |
| R(36) | 1126.3169 | 12 | R(37) | 1126.6478 | -4 | R(38) | 1126.8457 | 22 | R(39) | 1126.9031 | 19 |
| R(40) | 1126.8251 | 40 | R(41) | 1126.6033 | 5 | R(42) | 1126.2470 | 7 | R(43) | 1125.7552 | 43 |
| R(44) | 1125.1166 | -3 | R(45) | 1124.3445 | 7 | | | | | | |
| | | | | | (2, 1) Band | | | | | | |
| P(25) | 849.9878 | -21 | P(24) | 856.8586 | -8 | P(23) | 863.6636 | -11 | P(22) | 870.4041 | -2 |
| P(21) | 877.0755 | -10 | P(20) | 883.6786 | -10 | P(19) | 890.2112 | -9 | P(18) | 896.6719 | -3 |
| P(17) | 903.0584 | 0 | P(16) | 909.3687 | -4 | P(15) | 915.6027 | -1 | P(14) | 921.7581 | 4 |
| P(13) | 927.8322 | -1 | P(12) | 933.8261 | 10 | P(11) | 939.7351 | 6 | P(10) | 945.5587 | -4 |
| P(9) | 951.2968 | -3 | P(8) | 956.9476 | 4 | P(7) | 962.5077 | -1 | P(6) | 967.9777 | 2 |
| P(5) | 973.3553 | 6 | P(4) | 978.6383 | 3 | P(3) | 983.8272 | 12 | P(2) | 988.9140 | -33 |
| R(0) | 1003.5959 | -4 | R(1) | 1008.2855 | -11 | R(2) | 1012.8723 | -9 | R(3) | 1017.3544 | -6 |
| R(4) | 1021.7290 | -14 | R(5) | 1025.9983 | 0 | R(6) | 1030.1571 | -4 | R(7) | 1034.2064 | -3 |
| R(8) | 1038.1447 | 2 | R(9) | 1041.9701 | 0 | R(10) | 1045.6812 | -9 | R(11) | 1049.2794 | 1 |
| R(12) | 1052.7604 | -4 | R(13) | 1056.1250 | -3 | R(14) | 1059.3713 | -5 | R(15) | 1062.4990 | -3 |
| R(16) | 1065.5049 | -19 | R(17) | 1068.3931 | -1 | R(18) | 1071.1571 | -5 | R(19) | 1073.7987 | -4 |
| R(20) | 1076.3163 | -5 | R(21) | 1078.7088 | -9 | R(22) | 1080.9766 | -3 | R(23) | 1083.1170 | -9 |
| R(24) | 1085.1323 | 7 | R(25) | 1087.0178 | 4 | R(26) | 1088.7737 | -7 | R(27) | 1090.4009 | -11 |
| R(28) | 1091.9001 | 6 | R(29) | 1093.2664 | 2 | R(30) | 1094.5012 | -3 | R(31) | 1095.6043 | -5 |
| R(32) | 1096.5769 | 14 | R(33) | 1097.4123 | -10 | R(34) | 1098.1168 | -5 | R(35) | 1098.6866 | -7 |
| R(36) | 1099.1225 | -4 | R(37) | 1099.4225 | -9 | R(38) | 1099.5901 | 15 | R(39) | 1099.6178 | -3 |
| R(40) | 1099.5115 | -1 | R(41) | 1099.2704 | 17 | R(42) | 1098.8873 | -19 | R(43) | 1098.3707 | -22 |
| R(44) | 1097.7241 | 46 | | | | | | | | | |

for the correction to the Born–Oppenheimer breakdown on the hydrogen center. No $u$'s or $q$'s were statistically determined for the indium center, which is consistent with the Δ's on the indium center not being determined by the Dunham $U$ fits. The final standard deviation of the fit was 1.019, the dissociation energy $D_e$ was fixed to the InH value quoted in Ref. (*28*) (deduced from the observed predissociation in the $a^3\Pi$ state), and the atomic masses were taken from Ref. (*22*). It is also worth mentioning that the value of $R_e$ given in Table VIII, 1.8359670(8) Å, is in reasonably good agreement with the value, $R_e$ = 1.8359710(9) Å, derived from the Dunham $U_{01}$. The results in Table VIII are based on numerically integrating the radial Schrödinger equation in the range, 1.0 Å $\leq R \leq$ 3.2 Å, with a grid spacing of 0.0022 Å.

TABLE IV—*Continued*

| Line | Observed | Δ | Line | Observed | Δ | Line | Observed | Δ | Line | Observed | Δ |
|---|---|---|---|---|---|---|---|---|---|---|---|
| | | | | | (3, 2) Band | | | | | | |
| P(22) | 848.7266 | -5 | P(21) | 855.2707 | 2 | P(20) | 861.7464 | 6 | P(19) | 868.1507 | -9 |
| P(18) | 874.4866 | 4 | P(17) | 880.7481 | 1 | P(16) | 886.9349 | -7 | P(15) | 893.0478 | 5 |
| P(14) | 899.0816 | 2 | P(13) | 905.0378 | 11 | P(12) | 910.9099 | -14 | P(11) | 916.7032 | -7 |
| P(10) | 922.4132 | 3 | P(9) | 928.0366 | -2 | P(8) | 933.5751 | 10 | P(7) | 939.0245 | 12 |
| P(6) | 944.3838 | 8 | P(5) | 949.6502 | -16 | P(4) | 954.8299 | 18 | R(1) | 983.8272 | -394 |
| R(2) | 988.3587 | 16 | R(3) | 992.7470 | 28 | R(4) | 997.0277 | 10 | R(5) | 1001.2033 | 0 |
| R(6) | 1005.2720 | -9 | R(7) | 1009.2361 | 19 | R(8) | 1013.0854 | -5 | R(9) | 1016.8271 | 2 |
| R(10) | 1020.4554 | -7 | R(11) | 1023.9718 | -6 | R(12) | 1027.3744 | 0 | R(13) | 1030.6617 | 2 |
| R(14) | 1033.8323 | 1 | R(15) | 1036.8857 | 0 | R(16) | 1039.8208 | -2 | R(17) | 1042.6369 | -1 |
| R(18) | 1045.3328 | 0 | R(19) | 1047.9085 | 10 | R(20) | 1050.3596 | -6 | R(21) | 1052.6897 | -2 |
| R(22) | 1054.8958 | -2 | R(23) | 1056.9769 | -5 | R(24) | 1058.9337 | 3 | R(25) | 1060.7633 | -1 |
| R(26) | 1062.4660 | -4 | R(27) | 1064.0419 | 2 | R(28) | 1065.5049 | 161 | R(29) | 1066.8066 | -3 |
| R(30) | 1067.9972 | 17 | R(31) | 1069.0526 | -13 | R(32) | 1069.9810 | -5 | R(33) | 1070.7791 | 13 |
| R(34) | 1071.4442 | 19 | R(35) | 1071.9706 | -38 | R(36) | 1072.3684 | -53 | R(37) | 1072.6359 | -40 |
| R(38) | 1072.7734 | 10 | | | | | | | | | |
| | | | | | (4, 3) Band | | | | | | |
| P(18) | 852.6826 | 46 | P(17) | 858.8199 | 14 | P(16) | 864.8851 | -6 | P(15) | 870.8803 | 21 |
| P(14) | 876.7942 | -2 | P(13) | 882.6312 | -16 | P(12) | 888.3925 | 7 | P(11) | 894.0711 | 11 |
| P(10) | 899.6670 | 11 | P(9) | 905.1771 | -8 | P(8) | 910.6056 | 9 | P(7) | 915.9465 | 18 |
| P(6) | 921.1985 | 20 | P(5) | 926.3576 | -11 | R(4) | 972.7484 | 3 | R(5) | 976.8328 | -18 |
| R(6) | 980.8179 | 24 | R(7) | 984.6878 | -20 | R(8) | 988.4563 | 3 | R(9) | 992.1148 | 15 |
| R(11) | 999.0975 | 16 | R(12) | 1002.4185 | -8 | R(13) | 1005.6297 | 7 | R(14) | 1008.7260 | 17 |
| R(15) | 1011.7036 | -3 | R(16) | 1014.5667 | -2 | R(17) | 1017.3135 | 10 | R(18) | 1019.9391 | -4 |
| R(19) | 1022.4479 | 8 | R(20) | 1024.8375 | 31 | R(21) | 1027.0999 | -6 | R(22) | 1029.2449 | 3 |
| R(23) | 1031.2661 | 3 | R(24) | 1033.1614 | -18 | R(25) | 1034.9334 | -28 | R(26) | 1036.5857 | 16 |
| R(27) | 1038.1048 | -12 | R(28) | 1039.5028 | 15 | R(29) | 1040.7723 | 30 | R(30) | 1041.9112 | 18 |
| R(31) | 1042.9226 | 16 | R(32) | 1043.8044 | 9 | R(33) | 1044.5591 | 29 | R(35) | 1045.6812 | 106 |

TABLE V

Dunham $Y$ Constants (in $cm^{-1}$)

| | $^{115}$InH | $^{113}$InH | $^{115}$InD | $^{113}$InD |
|---|---|---|---|---|
| $Y_{10}$ | 1475.41832(54) | 1475.53193(54) | 1048.60513(44) | 1048.76510(44) |
| $Y_{20}$ | −25.142560(516) | −25.146432(516) | −12.700379(344) | −12.704254(344) |
| $Y_{30}$ | 0.233526(208) | 0.233580(208) | 0.085241(103) | 0.085280(103) |
| $10^3\ Y_{40}$ | −4.2632(377) | −4.2646(377) | −1.2986(106) | −1.2994(106) |
| $10^5\ Y_{50}$ | −5.931(251) | −5.934(251) | | |
| $Y_{01}$ | 4.99612491(219) | 4.99689434(219) | 2.52411049(323) | 2.52488066(323) |
| $Y_{11}$ | −0.14532724(176) | −0.14536082(176) | −0.05215818(109) | −0.05218206(109) |
| $10^3\ Y_{21}$ | 1.70892(121) | 1.70944(121) | 0.442482(686) | 0.442752(686) |
| $10^5\ Y_{31}$ | −2.7874(349) | −2.7885(349) | −0.6761(110) | −0.6766(110) |
| $10^6\ Y_{41}$ | −1.1016(344) | −1.1021(344) | | |
| $10^4\ Y_{02}$ | −2.2875166(621) | −2.2882212(621) | −0.5842442(738) | −0.5846008(738) |
| $10^6\ Y_{12}$ | 4.45973(252) | 4.46145(252) | 0.81813(126) | 0.81875(126) |
| $10^8\ Y_{22}$ | −4.448(145) | −4.450(145) | −1.0224(596) | −1.0233(597) |
| $10^9\ Y_{32}$ | −6.177(483) | −6.180(483) | −0.1757(957) | −0.1758(958) |
| $10^{10}\ Y_{42}$ | −1.259(534) | −1.260(534) | | |
| $10^9\ Y_{03}$ | 5.93889(737) | 5.94164(737) | 0.75290(520) | 0.75359(520) |
| $10^{11}\ Y_{13}$ | −6.723(127) | −6.727(127) | −0.934(140) | −0.935(140) |
| $10^{11}\ Y_{23}$ | −1.6980(313) | −1.6991(313) | | |
| $10^{13}\ Y_{04}$ | −1.9127(318) | −1.9139(318) | −0.0762(279) | −0.0763(279) |

TABLE VI

Dunham $U$ Constants (in $cm^{-1}$)

| | unconstrained | constrained |
|---|---|---|
| $U_{10}$ | 1475.85435(41) | 1475.85423(41) |
| $U_{20}$ | -25.143564(410) | -25.143161(427) |
| $U_{30}$ | 0.234114(179) | 0.233691(190) |
| $10^3$ $U_{40}$ | -4.4242(330) | -4.3102(353) |
| $10^5$ $U_{50}$ | -4.788(224) | -5.776(238) |
| $U_{01}$ | 5.00105645(825) | 5.00109284(494) |
| $U_{11}$ | -0.14532119(170) | -0.145329078(783) |
| $10^3$ $U_{21}$ | 1.70590(123) | 1.714950(437) |
| $10^5$ $U_{31}$ | -2.7884(369) | -3.0289(123) |
| $10^6$ $U_{41}$ | -1.0896(374) | -0.8986(129) |
| $10^4$ $U_{02}$ | -2.296396(204) | -2.297036 |
| $10^6$ $U_{12}$ | 4.44863(264) | 4.453961 |
| $10^8$ $U_{22}$ | -4.405(154) | -5.229765 |
| $10^9$ $U_{32}$ | -6.196(528) | -4.885510 |
| $10^{10}$ $U_{42}$ | -1.231(588) | -1.321549 |
| $10^9$ $U_{03}$ | 6.0720(130) | 6.021433 |
| $10^{11}$ $U_{13}$ | -6.651(139) | -4.916882 |
| $10^{11}$ $U_{23}$ | -1.7052(346) | -1.304030 |
| $10^{13}$ $U_{33}$ | | -4.117747 |
| $10^{13}$ $U_{04}$ | -1.9323(360) | -1.887975 |
| $10^{15}$ $U_{14}$ | | -8.579189 |
| $10^{16}$ $U_{24}$ | | -1.924400 |
| $10^{17}$ $U_{34}$ | | -4.160903 |
| $10^{18}$ $U_{05}$ | | 8.030991 |
| $10^{19}$ $U_{15}$ | | -5.548885 |
| $10^{19}$ $U_{25}$ | | -1.447476 |
| $10^{22}$ $U_{06}$ | | -5.426528 |
| $10^{24}$ $U_{16}$ | | -8.395688 |
| $10^{24}$ $U_{26}$ | | 6.935906 |
| $10^{26}$ $U_{07}$ | | 1.317535 |
| $10^{27}$ $U_{17}$ | | -9.436134 |
| $10^{30}$ $U_{08}$ | | -1.216152 |
| $10^{31}$ $U_{18}$ | | 7.238908 |
| $10^{35}$ $U_{09}$ | | -3.697646 |
| $10^{39}$ $U_{010}$ | | 2.484912 |

A plot of the Born–Oppenheimer potential (Eq. (6)) is displayed in Fig. 1. Also included in this plot for the purpose of comparison is the theoretical internuclear potential for the $X\,0^+$ state obtained from a CI relativistic pseudopotential calculation by Teichteil and Spiegelmann (*15*). In order to carry out this comparison, the theo-

TABLE VII

Born–Oppenheimer Breakdown Parameters

| | unconstrained | constrained |
|---|---|---|
| $\Delta_{10}$ | -1.401448(356) | -1.401945(393) |
| $\Delta_{20}$ | -1.63708(606) | -1.65059(686) |
| $\Delta_{01}$ | -3.53217(323) | -3.54798(204) |
| $\Delta_{11}$ | -2.5037(103) | -2.52098(882) |
| $\Delta_{02}$ | -10.487(171) | -11.2522(264) |
| $\Delta_{12}$ | | -4.751(131) |
| $\Delta_{03}$ | -43.24(377) | -39.276(527) |

TABLE VIII

Fitted Potential Parameters for the Modified Morse Form of the Internuclear Potential (Eqs. (6), (9), and (10))

| | |
|---|---|
| $D_e$ ($cm^{-1}$) | 20730. |
| $R_e$ (Å) | 1.835967012(825) |
| $\beta_0$ | 4.58365269(279) |
| $\beta_1$ | 3.9542876(470) |
| $\beta_2$ | 7.752876(603) |
| $\beta_3$ | 17.39880(574) |
| $\beta_4$ | 34.0867(734) |
| $\beta_5$ | 50.942(428) |
| $\beta_6$ | 72.47(331) |
| $\beta_7$ | 768.4(157) |
| $\beta_8$ | 380.5(245) |
| $u_1^H$ ($cm^{-1}$ Å$^{-1}$) | -115.8569(593) |
| $u_2^H$ ($cm^{-1}$ Å$^{-2}$) | 181.919(116) |
| $u_3^H$ ($cm^{-1}$ Å$^{-3}$) | -182.138(951) |
| $u_4^H$ ($cm^{-1}$ Å$^{-4}$) | 128.01(246) |
| $u_5^H$ ($cm^{-1}$ Å$^{-5}$) | -48.43(197) |
| $10^3 q_1^H$ | 1.13326(412) |
| $10^3 q_2^H$ | -2.6909(392) |
| $10^3 q_3^H$ | 2.9557(572) |
| $10^3 q_4^H$ | -1.5326(334) |
| $M_A$ ($^{113}$In) | 112.904061 |
| $M_A$ ($^{115}$In) | 114.903882 |
| $M_B$ (H) | 1.007825035 |
| $M_B$ (D) | 2.014101779 |

retical potential from Ref. (*15*), tabulated in terms of total energy, had to be transformed to the dimensionless $0 \leqslant V(R)/D_e \leqslant 1$ energy scale using the procedure described in Ref. (*29*). The pseudopotential calculation yielded a value of $R_e = 1.86$

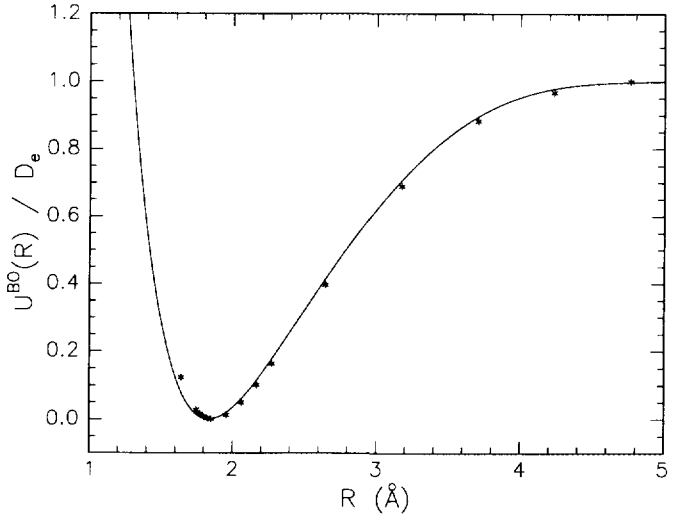


FIG. 1. Direct comparison of our indium hydride Born–Oppenheimer potential (solid curve) with the theoretical pseudopotential (discrete points) reported by Teichteil and Spiegelmann (*15*).

Å (3.52 au) for the equilibrium internuclear separation, as compared to 1.84 Å (3.47 au) from our potential fit. Even apart from this minor shift in the minimum of these potentials, the outer wall of our potential is shifted noticeably toward shorter internuclear separation and is slightly steeper than the theoretical potential.

The only other theoretical calculation performed on InH was the CASSCF calculation by Balasubramanian (*16*). Unfortunately, the author failed to provide a tabulated list of potential energy curve values for the $X\,^1\Sigma^+$ state and, therefore, a comparison with our potential is impossible.

ACKNOWLEDGMENTS

This work was supported by the Natural Sciences and Engineering Research Council of Canada (NSERC). Acknowledgement is made to the Petroleum Research Fund, administered by the American Chemical Society, for partial support of this work.

RECEIVED: August 16, 1994

REFERENCES

1. B. GRUNDSTRÖM, *Nature* **141,** 555 (1938).
2. B. GRUNDSTRÖM, *Z. Phys.* **113,** 721–729 (1939).
3. B. KLEMAN, Dissertation, Stockholm, 1953.
4. H. NEUHAUS, *Z. Phys.* **150,** 4–9 (1958).
5. H. NEUHAUS, *Z. Phys.* **152,** 402–416 (1958).
6. M. L. GINTER, *J. Mol. Spectrosc.* **11,** 301–320 (1963).
7. M. L. GINTER, *J. Mol. Spectrosc.* **20,** 240–247 (1966).
8. M. L. GINTER AND R. BATTINO, *J. Chem. Phys.* **42,** 3222–3229 (1965).
9. L. VESETH AND A. LOFTHUS, *J. Mol. Spectrosc.* **49,** 414–422 (1974).
10. T. LARSSON AND H. NEUHAUS, *Ark. Fys.* **27,** 275–287 (1964).
11. T. LARSSON, H. NEUHAUS, AND N. ÄSLUND, *Ark. Fys.* **37,** 141–149 (1967).
12. N. MUSTELIN, Thesis, Åbo, Finland, 1963.
13. K. FREED, *J. Chem. Phys.* **45,** 1714–1722 (1966).
14. L. VESETH, *J. Mol. Spectrosc.* **59,** 51–62 (1976).
15. C. TEICHTEIL AND F. SPIEGELMANN, *Chem. Phys.* **81,** 283–296 (1983).
16. K. BALASUBRAMANIAN, *J. Phys. Chem.* **94,** 6583–6588 (1990).
17. A. H. BAHNMAIER, R. D. URBAN, AND H. JONES, *Chem. Phys. Lett.* **155,** 269–272 (1989).
18. R. D. URBAN, H. BIRK, P. POLOMSKY, AND H. JONES, *J. Chem. Phys.* **94,** 2523–2531 (1991).
19. J. B. WHITE, M. DULICK, AND P. F. BERNATH, *J. Chem. Phys.* **99,** 8371–8378 (1993).
20. J. M. CAMPBELL, M. DULICK, D. KLAPSTEIN, J. B. WHITE, AND P. F. BERNATH, *J. Chem. Phys.* **99,** 8379–8384 (1993).
21. M. LOETE, J. HILICO, A. VALENTIN, J. CHAZELAS, AND L. HENRY *J. Mol. Spectrosc.* **99,** 63–86 (1983).
22. I. MILLS, T. CVITAS, K. HOMANN, N. KALLAY, AND K. KUCHITSU, "Quantities, Units, and Symbols in Physical Chemistry," Blackwell, Oxford, UK, 1989.
23. J. L. DUNHAM, *Phys. Rev.* **41,** 721–731 (1932).
24. A. H. M. ROSS, R. S. ENG, AND H. KILDAL, *Opt. Commun.* **12,** 433 (1974).
25. J. K. G. WATSON, *J. Mol. Spectrosc.* **80,** 411–421 (1980).
26. J. OGILVIE, *Comput. Phys. Commun.* **30,** 101–105 (1983) and private communication.
27. T. KARKANIS, M. DULICK, Z. MORBI, J. B. WHITE, AND P. F. BERNATH, *Can. J. Phys.*, in press.
28. K. P. HUBER AND G. HERZBERG, "Constants of Diatomic Molecules," Van Nostrand-Reinhold, New York, 1979.
29. H. G. HEDDERICH, M. DULICK, AND P. F. BERNATH, *J. Chem. Phys.* **99,** 8363–8370 (1993).